Electrical insulation performances of ceramic materials developed for advanced blanket systems under intense radiations

Electrical Insulation Performances of Ceramic Materials Developed for Advanced Blanket Systems under Intense Radiations

Teruya Tanaka [1], Takumi Chikada [2], Tatsuya Hinoki [3], Takeo Muroga [1]

[1] *National Institute for Fusion Science, Toki, Gifu 509-5292, Japan*
[2] *Shizuoka University, Shizuoka 422-8529, Japan*
[3] *Open Innovation Institute, Kyoto University, Uji, Kyoto 611-0011, Japan*

Abstract

Various oxides and SiC have been proposed as candidate materials for electrical insulation coatings and inserts to suppress the magnetohydrodynamic (MHD) pressure drop in liquid metal fusion blanket systems. From the early stage of the MHD insulator development, the magnitudes of the radiation-induced conductivities (RICs), i.e., increases in conductivities by radiation excitation, have been evaluated on bulk and coated specimens by using several radiation sources. While the insulating performances of the oxide coated and SiC plate specimens are inferior to those of high quality and purity bulk materials due to cracks, pits, sintering additives, etc., the results indicate that the RIC phenomenon would not prevent the MHD insulators from achieving the required performances (10^{-3}-10^{-2} S/m for coatings, 10^{2} S/m for inserts) at the first wall of the blanket (500–700℃, several kGy/s). The recent design investigation of blanket modules for DEMO reactor conditions provides more precise information for prediction of the performances in reactors and conditions to be simulated in the future irradiation damage studies. In the case of the coatings, the suppression of recoiled Li from the liquid metal breeder/coolant might be an issue to be considered in the development.

.

Keywords: Ceramic materials, electrical insulation, liquid metal blanket, radiation induced conductivity, recoil atoms

Highlights

Corresponding author: Teruya Tanaka / tanaka.teruya@nifs.ac.jp

- Oxide and SiC materials are developed for MHD insulators in liquid metal blanket.
- Electrical insulating performances at high temperatures could satisfy requirements.
- Radiation induced conductivity phenomenon would not be an issue in development.
- In addition to irradiation damage, there is concern about injection of recoil atoms.

1 Introduction

In the development of advanced liquid metal (such as LiPb and Li) blanket systems, the suppression of the MHD pressure drop in a breeder/coolant flowing under intense magnetic fields is required to avoid significantly heavy loads on circulation pumps. For this purpose, the development of ceramic electrical insulators has been conducted as one of the essential tasks in the development of blanket systems [1-3]. Various oxides (Er_2O_3, Y_2O_3, $CaZrO_3$, ZrO_2, etc.) and SiC have been proposed as candidate insulating materials from the viewpoint of chemical stability of the materials [4, 5]. Although their initial electrical conductivities at room temperature can satisfy the required insulation performances ($<10^{-3}$–10^{-2} S/m for coatings and $<10^{2}$ S/m for inserts) with adequate margins, the magnitudes of the conductivities will increase significantly by thermal excitation of charge carriers at high temperatures and by radiation excitation in an intense radiation environment, i.e., radiation-induced conductivity (RIC) phenomenon. Since it is considered difficult to suppress those increases in conductivities significantly by material modification, several RIC measurements at high temperatures have been conducted at the early stage of the MHD insulator development. The results and impacts on blanket designs are described comprehensively in the present paper.

Following the RIC evaluations, various fabrication techniques of the insulating layers which could be applied for large and complicated blanket structures have been studied and their performances have also been evaluated. Recent design studies on the liquid metal blanket modules for DEMO reactor conditions enable more precise predictions of the insulation performances of the MHD insulators in reactor environments. The influence of irradiation damage effects, i.e., radiation-

Corresponding author: Teruya Tanaka / tanaka.teruya@nifs.ac.jp

induced electrical degradation (RIED) phenomenon, could also be discussed based on results of the previous irradiation experiments performed on various Al_2O_3 materials for the ITER diagnostic systems, etc. In the use of coatings in fusion reactors, injection of recoil Li atoms from liquid metal coolants might be a problem in maintaining the required performances during a lifetime of a blanket module.

At the beginning, structures of the liquid metal-cooled blanket modules tentatively proposed in Japan are introduced to indicate the considered requirements and usage conditions.

2. Self-cooled liquid metal blanket modules

2.1 Present design investigation in Japan

Universities and the National Institute for Fusion Science (NIFS) in Japan have conducted studies on technologies of advanced liquid blanket systems for high-efficiency power generation at > 500 ℃ [6–8]. Especially, the studies focus on self-cooled blanket systems, because of their merits, such as simple blanket structures and low-pressure circulation systems. In the blanket systems, a liquid metal (such as Li and LiPb) or a molten salt (such as FLiBe and FLiNaBe) circulates as a tritium fuel breeder and coolant (breeder/coolant). In the following sections, two structures of the self-cooled liquid metal blanket modules, which have tentatively been proposed for DEMO relevant conditions, are introduced. These are the references which provide the environmental information that should be considered in the present development of MHD insulators.

2.2 Blanket module for a helical reactor

One of the liquid blanket module designs investigated at present is the LiPb and Li blankets for the helical reactor FFHR-d1 [9]. The fusion power of the reactor is 3GW and the average neutron wall loading is 1.5 MW/m^2. The magnitude of the neutron wall loading is similar to that of the tokamak JA-DEMO reactor described below. Figure 1 shows the cross section of the cartridge type

blanket module for FFHR-d1 [10, 11]. Since the average heat load from the core plasma is estimated to be considerably low, i.e., 0.1 MW/m^2, long channels could be applicable to the cooling of the first wall. The preliminary thermo-fluid analysis, including the MHD effects on the liquid metal flow, was performed using the STREAM code [12]. Since the thicknesses of the meshes near the channel walls must be significantly less to estimate the MHD pressure drop [13], a straight channel geometry was assumed in the calculation. The results indicated that the average velocity of the LiPb flow would be ~1.4 m/s to maintain the temperature of the first wall at <550°C, which is the maximum allowable temperature for the reduced activation ferritic/martensitic (RAFM) steel. Due to the strong magnetic field of 2.5–7.5 T in the blanket region, the magnitude of the MHD pressure drop is estimated to be ~110 MPa when the LiPb flows through the metal coolant channels. If all the channel walls are electrically insulated, the pressure drop is suppressed to ~0.4 MPa. The voltages applied to the insulating layers, which are the one of important parameters in examination of the dielectric strength characteristics of candidate materials and irradiation effects, are calculated to be ~0.3 V. Also, the three-surface insulation [14, 15] could suppress the pressure drop to a similar magnitude, and the voltages are ~0.5 V.

2.3 Test blanket module in DEMO reactor

Another investigated liquid metal blanket system is a test blanket module for JA-DEMO (DEMO-TBM) [16]. In the Japanese DEMO reactor, a demonstration of power generation will be performed using a water-cooled ceramic breeder (WCCB) blanket system [17, 18]. While the details remain undecided, technology validation of the advanced blanket systems is proposed to be performed by installing a test blanket module in the late operation period. Figure 2 shows the self-cooled LiPb DEMO-TBM for JA-DEMO tentatively proposed at present [19]. The dimensions of the module are the same as those of the WCCB blanket module. The heat load from the core plasma is ~0.5 MW/m^2 and the maximum neutron wall loading is 1.5 MW/m^2 in the JA-DEMO design. Since the first wall cooling channels are almost parallel to the magnetic field, MHD insulators

would be unnecessary. The MHD insulator is considered necessary for the side flow channels and coolant ducts in the manifold regions. The maximum magnetic field in the blanket region is ~10 T in JA-DEMO. The average velocity is ~0.18 m/s at the side flow channels and the magnitude of the MHD pressure drop is calculated to be ~5 MPa without electrical insulation. The voltages applied to the insulating layer are ~0.05 V. In the coolant ducts in the manifold regions, the average velocity is 1.9 m/s. The magnitude of the MHD pressure drop is calculated to be ~400 MPa without electrical insulation. The voltage applied to the insulating layer is ~1.7 V. Since a heat removal function is not needed in these coolant ducts, insulating inner pipes could be installed to suppress the MHD pressure drop instead of coatings.

3. Required performance of MHD insulators and candidate materials

Fundamental experimental and theoretical studies on the MHD effects in a liquid metal coolant flowing under a strong magnetic field have been conducted for many decades [20-22]. For the metal channels where heat removal is necessary, insulating coatings could suppress magnitudes of the MHD pressure drop with high heat removal performances. For the coolant ducts behind the blanket modules where a high-performance heat removal is not necessary, robust MHD insulating inserts, i.e., inner plates or pipes, would be applicable.

The required insulating performances for ceramic coatings with ~10 μm thickness are considered $< 10^{-2}$ S/m from the calculations in Ref. 15. The analysis showed that the MHD pressure drop could be suppressed by more than 2 orders with insulating coatings. Since the considered thickness is mainly ~1 - 10 μm in our development activities, the target of the development is to maintain the electrical conductivities at $<10^{-3}$ - 10^{-2} S/m. For the MHD insulating inserts called flow channel inserts (FCIs) with several mm in thickness, the allowable electrical conductivity would be 100 S/m [23]. To achieve the same electrical insulating performance with a thinner coating, a higher electrical resistivity (i.e., lower conductivity) is required for the material.

Candidate materials are selected from the viewpoint of chemical compatibility in liquid Li and LiPb breeder/coolants [4, 5]. In Japan, the studies have been conducted with Er_2O_3, Y_2O_3, $CaZrO_3$, etc. for Li blanket systems [24], and SiC for LiPb blanket systems [25]. Recently, ZrO_2 [26], MgO, Al_2O_3 [27], etc. are also being studied for LiPb the blanket systems.

4. Initial insulation performances of MHD insulators

Universities and NIFS in Japan have studied several coating techniques for fabricating MHD insulators in liquid metal blanket modules [3, 24, 25]. Regarding the performance evaluations of the coatings, those fabricated by the metal-organic decomposition (MOD) method have been examined intensively. Since this method is a liquid-phase process, it is considered suitable for fabricating large-area coatings in complicated blanket structures with thicknesses less than several μm [28]. In large-area coating layers fabricated by this method, cracks and pits degrades the insulation performances compared with those of sintered ceramic bulk materials. Furthermore, in the fabrication process of coatings, the maximum heat treatment temperatures are limited to avoid degrading the properties of the structural materials, e.g., <~700 ℃ for coatings on RAFM steel substrates [29]. Therefore, the initial crystallinities of the coatings degrade compared with those of sintered ceramic materials. This trend could also be a factor that degrades the insulating performances. However, considering the required insulation performances for suppression of MHD pressure drop, the large-area MOD coatings could achieve adequate electrical insulation performances. Regarding the dielectric strength, a 1-μm thick MOD Er_2O_3 coating showed strength of ~20 kV/mm at room temperature [28], and a recent evaluation on a 2-μm thick MOD MgO coating showed the strength of >35 kV/mm at 500 ℃.

Robust MHD insulating inserts [25, 30, 31] have been developed with SiC materials. The evaluated initial electrical conductivities of sintered SiC materials exceeded those of oxide materials. This is considered that the sintering additives affected the conductivities.

The temperature dependence of the electrical conductivities of the Er_2O_3 coatings, MgO coatings and sintered 3C-SiC plates are shown in Fig. 3 [28, 32, 33]. Those of the sintered Er_2O_3 disk and single-crystal 4H-SiC plates are also plotted for comparison. The increases in the conductivities with temperature are proportional to $\exp(-E_a/k_BT)$ if the dominant mechanism that determines the conductivities does not change with temperature. Here E_a is the activation energy, k_B is the Boltzmann constant and T is the temperature. In insulators that show significantly high insulation performances (lower conductivities) at room temperature, the conductivities increase with large activation energies. If the increase in the conductivity is dominated by the band gap energy, it is approximately proportional to $\exp(-E_g/2k_BT)$, where E_g is the band gap energy [34]. The curve fitting of the conductivity of the 4H-SiC plate at T> 200 ℃ gives E_g =3.4 eV, which is close to the band gap energy appeared in the literature [35].

The sintered Er_2O_3 disk and single-crystal 4H-SiC plate showed high insulation performances (low conductivities) at room temperature, and their conductivities increased significantly at high temperatures. However, in the insulators that showed lower insulation performances (higher conductivities) at room temperature, their conductivities increased with smaller activation energies. While the conductivities of the oxide materials and SiC plates spread 7 orders and 4 orders of magnitude at low temperatures, respectively, they converge into the ranges of ~2 orders at the blanket temperatures of 500–700 ºC, i.e., 10^{-4}-10^{-6} S/m for oxides and 10^{-1}-10^{1} S/m for SiC plates, respectively.

5. Evaluation of Radiation Induced Conductivities

5.1 Dose rate under DEMO conditions

The neutron wall loadings on the blanket modules described in the Sections 2.2 and 2.3 are ~1.5 MW/m^2 (14 MeV neutron current from a core plasma: 6.6 x 10^{13} n/cm^2/s), and almost twice of that in ITER [36]. The radiation energy depositions at the first wall were calculated for the candidate

materials by using the neutron and gamma-ray transport code MCNP-6 [37] and a simple torus model. In Fig. 4, the energy depositions in the candidate materials are plotted with the unit of dose rate (Gy/s = J/kg/s). Even in the same neuron and gamma-ray environment, the dose rates differ among the materials [38], and they range from ~1 to 3 kGy/s. The dose rate at the rear side of the 60-cm thick LiPb blanket module is ~1/50.

5.2 Radiation induced conductivity

When an insulator is irradiated, electrons in the valence band are excited to the conduction band beyond the band gap [34]. The excited electrons drift in the material due to the electrical field until they are captured to defects, impurity levels or holes (recombination). In high-quality semiconductor materials, holes might also drift. This drift of electrons and holes (charge carriers) increases the conductivity, i.e., radiation induced conductivity (RIC) [34]. The RIC magnitude is determined by the number of produced charge carriers and their drift distances. In the semiconductor materials, the energy to produce an electron-hole pair is approximately three times the band gap energy [38]. The energy for the pair production (75 eV) and mobilities of charge carriers in Al_2O_3 are shown and discussed in Refs. 39 and 40. RICs appear only during irradiation.

5.3 Evaluation of Radiation induced conductivities

Profound evaluations and studies of RICs have previously been conducted on Al_2O_3, MgO, etc. and those included evaluations for the diagnostics systems of ITER [41-44]. The present evaluation of RICs for the MHD insulators follows those methods and discussions. A series of the evaluations have been performed using a DT neutron source, ^{60}Co gamma-ray source and material testing fission reactor. In the evaluations, the typical dimensions were 10 mm diameter × 1 mm thick, 10 mm × 10 mm × 0.4 -1.0 mm thick, etc. for plate specimens. The coated specimens were fabricated on 15 mm x 15 mm x 2 mm thick stainless steel plates with 1-2 μm thick coating layers, and the

conductivities were evaluated by 2-4 mm^2 electrodes on the coated surfaces. The RIC evaluations were performed in vacuum chambers to suppress background electrical currents due to the ionized atmospheric gasses except for the fission reactor experiment.

Several results of the RIC measurements under ^{60}Co gamma-ray irradiation are shown in Fig. 5 [32, 33]. The measurements were performed to examine the relations between conductivity increases by radiation excitation and thermal excitation. The conductivities of the sintered Y_2O_3 disk and single-crystal 4H-SiC plate without irradiation were ~10^{-14} S/m and significantly low at room temperature. During irradiation, they increased to ~3×10^{-10} S/m and ~1×10^{-7} S/m, respectively. The differences in the conductivities under and without irradiation correspond to the RICs. The temperature dependence indicates that the magnitudes of the RICs do not change significantly with temperature. At high temperatures, the increases in the conductivities by thermal excitation are dominant. These results indicate that the effects of radiation excitation and thermal excitation are almost independent from the viewpoint of the MHD insulator development. In the MOD Er_2O_3 coating and 3C-SiC plates with high initial conductivities, differences in conductivities under and without irradiation, i.e., RICs, were negligible at all temperatures.

Figure 6 shows the dose rate dependence of RICs obtained by our research group at low temperatures of < 50 ℃ [28, 32, 33, 45–47]. Similar to previous results for Al_2O_3 materials, the magnitudes of RICs in the MHD insulators also increase almost in proportion to the dose rate. Since the single-crystal 4H-SiC has low impurities and defect densities for semiconductor device development, the high RIC is considered due to the long drift distances of charge carriers in the crystal. Regarding the sintered 3C-SiC materials studied for fusion reactors, the magnitudes of RICs are considered <1.6×10^{-8} S/m because the accurate measurement was difficult due to the high inherent conductivity (initial conductivity without irradiation). The RICs were measured on Er_2O_3 coated specimens fabricated at 400–600 ℃ to prevent property degradation of the structural material as described in Section 4. The smaller magnitudes of RICs are considered due to the

shorter drift distance of charge carriers as a result of the lower crystallinity. Except for the fission reactor experiment in which the specimens were broken or electrodes were disconnected during the reactor operation, it has been confirmed that the increases of the electrical conductivities due to the RIC phenomenon were appeared only during irradiation and the conductivities returned to the initial levels after stopping irradiation.

5.4. Impact of radiation induced conductivities

The changes in the conductivities with temperature, the magnitude of the RICs estimated for the DEMO relevant condition and the required insulation performances are illustrated in Fig. 7. Compared with Al_2O_3 materials previously studied for diagnostic systems, temperatures and irradiation damages will be higher in the blanket environment. On the other hand, the requirements for insulation performances of the MHD insulators (10^{-3}–10^{-2} S/m for coatings, 100 S/m for inserts) are considerably moderate compared with those of Al_2O_3 materials for diagnostics (~10^{-6} S/m for ~100 Gy/s [48]). The magnitudes of the RIC effects would be ~10^{-6} S/m in oxide materials and <~1×10^{-5} S/m in sintered SiC materials under the dose rates of several kGy/s at the first walls of blanket modules. The results of the series of RIC measurements indicate that the increase in the conductivities due to the RIC effect would not be an issue in the development of the MHD insulator.

As described in Section 4, the increases in the conductivities due to thermal excitation are dominant at blanket temperatures of 500–700 °C, and the conductivities are 10^{-4}–10^{-6} S/m for oxide materials and 10^{-1}–10^{1} S/m for SiC materials, respectively. These conductivities are the initial performances of the MHD insulators at the start of use in the blanket modules. During reactor operations, the degradation of the performances due to irradiation damage, etc. should be suppressed within 1-3 orders both in the oxide and SiC materials to maintain the required performances.

6. Issues concerning irradiation damage

6.1 Irradiation damage under DEMO relevant conditions

Magnitudes of the irradiation damages of the MHD insulators at a first wall of a blanket module are calculated as shown in Fig. 8 using the same method as the dose rate calculation in Section 5.1. Except for SiC, the displacement energy and efficient factor assumed in the calculations are 40 eV and 0.8, which are similar to those of Fe materials. The displacement energy for SiC is assumed to be 28 eV [49]. The parameters for ceramic materials are discussed in Ref. 40. When the damage reaches 100 dpa (displacement per atom) in a RAFM steel (reduced activation ferritic/martensitic steel), those in the ceramic materials are calculated to be ~100 dpa. At the rear side of the breeding blanket region, those decrease to ~1/20.

6.2 Irradiation damage and applied electric field strength

In the previous profound studies on Al_2O_3 materials, permanent degradation in electrical insulation performances due to irradiation damage, i.e., radiation induced electrical degradation (RIED), has also been studied by various irradiation experiments. While the neutron irradiation of ~3 dpa showed no significant conductivity increases in Al_2O_3 materials [50], the RIED effect was observed in the ion beam irradiation [51]. In those studies, the temperature and electric field were considered important parameters that cause the RIED phenomenon. Refs. 52 and 53 proposed 200℃–600 ℃ and > 50 V/mm as the conditions that enhance RIED significantly (RIED danger area). The production of Al colloids in the Al_2O_3 materials has been discussed as the mechanism of degradation in insulation performance [54].

Regarding the MHD insulators, it has been reported that no significant increase in the electrical conductivities of SiC materials has been observed after fission neutron irradiation of 8 dpa [55]. For the MHD oxide coating materials (Er_2O_3, Y_2O_3, etc.), irradiation damage studies on the electrical insulation performances are considered few so far, except for some ion beam irradiations at room

temperature [56, 57]. Since various candidate materials and fabrication techniques are being studied, it is planned to perform a series of ion beam irradiations on ~1-μm thick coating layers to investigate the conductivity changes due to the irradiation damage and their relations with the temperature and strength of the applied electric field. The estimated ranges of several hundreds of keV proton beams and ~5 MeV heavy ion beams are > 1 μm. Penetration of the ion particles enables evaluations of conductivity changes in damaged ceramic materials. A damage rate of several dpa/h can be provided by the ion beam irradiation and changes in the insulating performances up to 100 dpa could be examined as shown in the development of structural materials [58]. In the experiments, the adhesion properties between the ceramic and metal layers under irradiation at high temperatures could also be examined.

If the electric field strength of 50 V/mm proposed in the irradiation damage studies on Al_2O_3 materials [52, 53] is referred to as a criterion, the ~10-μm thick insulating coatings could suppress the field strength to the criterion in the cooling channels inside the blanket modules shown in Sections 2.2 and 2.3. Since the field strengths applied on the insulating coatings are approximately proportional to channel widths, those could be mitigated by reducing the channel widths and increasing the number of channels in the blanket design.

7. Radioactivities of insulator materials

In the insulator material selection, a magnitude of radioactivity is often a discussed topic. The reduction of aluminum impurity producing ^{26}Al (half-life $T_{1/2}$: 7.4 x 10^5 years) is required in the development of low-activation structural materials [59]. In the use of Er_2O_3, the production of ^{166m}Ho ($T_{1/2}$: 1200 years) would be a concern. Figure 9 shows the contact dose rates of the RAFM steel F82H and the impacts of radioactivities of 5-μm thick insulator coatings calculated by FISPACT-II [60]. After 7.5 years of usage at the first wall of a LiPb blanket module, i.e., ~100 dpa in F82H, the dose rate of F82H without impurities drops to ~ 1×10^{-5} Sv/h by 100-year cooling. The

magnitude of the dose rate increases by 20 times in the calculation including the impurities provided in Ref. 61. The dose rate for 10 mm thick F82H with a 5-μm thick Al_2O_3 coating was calculated by considering a uniformly mixed material composition, i.e., F82H + 0.026 wt% Al_2O_3. This result indicates that the Al_2O_3 coating increases the dose rate slightly. However, the impact is smaller than that of the impurity elements in F82H. The magnitude of the dose rate of a 5-μm thick Er_2O_3 coating is almost the same level as those of the impurities in F82H. The impacts of radioactivities of MgO, Y_2O_3 and ZrO_2 coatings could be negligible in the usage with F82H.

8. Concerns on recoil atom injection in 14 MeV neutron environment

For coolant channels where a heat removal function is required, e.g., coolant channels of the first wall, the fabrication of thinner insulating coatings on metal channel walls might be preferable from the viewpoint of efficient cooling. However, the minimum thickness of the insulating layers might be limited by the range and behaviors of recoil atoms that are injected into the coating layers by 14 MeV neutrons (Fig. 10(a)). When a lithium atom is recoiled by elastic scattering with a 14 MeV neutron, the maximum energy of the recoil Li atom is 6.9 MeV and the corresponding range is estimated to be ~10 μm in a Y_2O_3 layer using the SRIM code [62]. The distribution of the Li atoms recoiled from a pure Li coolant flow and injected into a Y_2O_3 layer was calculated using the PHITS [63] code which can calculate the transport of neutrons and secondary charged particles produced by nuclear reactions. First, the energy spectrum of neutrons entering the first wall coolant channel from the core plasma side was calculated in the simple torus model shown in Fig. 4(a). Neutrons with the obtained spectrum were injected into the Li and Y_2O_3 layers with random angles between −85° and 85°(Fig. 10(b)).

The calculated distribution of the recoil Li atoms in the Y_2O_3 layer is shown in Fig. 10(c). In this distribution profile, it is assumed that the injected recoil Li atoms do not move during the operation by thermal diffusion and collisions of particles, i.e., initial positions of the injected Li atoms. While

a small part of the Li atoms reaches ~10 μ m from the surface of the Y_2O_3 layer due to the range of a recoil Li atom described above, most of the recoil Li atoms are observed up to 6–7 μ m from the surface. After 7.5 years of using a blanket module, the atomic concentration at the surface is calculated to be ~14 %. The distribution of Li atoms is calculated also for a combination of a LiPb coolant and Y_2O_3 layer. Due to the lower Li content and shorter range of the recoil Li atoms in the LiPb coolant, the Li concentration at the surface is calculated to be ~1.8 %. The influences of the injected recoil Li atoms on the electrical insulation performances have not been examined and experimental studies are considered required. Since the concentration of Li atoms in the coating layer is estimated to be considerably higher than those of the impurities, the insulation performance could be degraded significantly.

To suppress the injection of recoil Li atoms into the insulating coating layer, the multilayer coating technique could be effective (Fig. 11(a)). This technique attaches an Fe layer of 10–25 μm in thickness on the surface of the insulating layer [15]. The thickness of the Fe layer is limited to prevent the performance degradation as an insulating wall for reduction of the MHD pressure drop. The original purpose of the Fe layer attachment was to eliminate the penetration of the liquid metal through cracks in the coating layer [15]. Recently, the effectiveness as the anti-corrosion surface layer was pointed out and the preferable anti-corrosion performance of an Fe-ZrO_2-F82H (F82H is a substrate plate) multilayer specimen has been shown in corrosion tests in LiPb [64]. Since the range of a Li atom recoiled by a 14 MeV neutron with the maximum energy of 6.9 MeV is estimated to be 6.8 μm in Fe, the Fe inner layer can stop the recoil Li atoms.

Instead of the recoil Li atoms, Fe atoms are recoiled from the Fe inner layer and injected into the coating layer as shown in Fig. 11(b). The maximum energy and corresponding range are ~1 MeV and ~0.6 μm. The Fe concentration at the boundary (A) after 7.5 years of operation is calculated to be ~12 %. From the boundary (A), Cr atoms, which are produced by Fe(n, α)Cr nuclear reactions, are also injected. Although the concentration in the coating layer is considerably low (<~0.06 %),

the maximum energy and corresponding rage are ~2 MeV and ~1.2 μ m. In addition, metal atoms are recoiled and injected from the F82H (Fe-8Cr-2W) metal wall through the boundary (B). The major atoms are Fe and Cr. Those maximum energies and corresponding ranges are same as those injected from the boundary (A) as described above. Their calculated concentrations at the boundary (B) are ~8 % and ~1 %, respectively. Since the neutrons are backscattered in the blanket and transported in all directions as illustrated in Fig. 11(b), the influence of backscattered neutrons is included in the concentration evaluations of recoil metals from the Fe inner layer and F82H wall.

The minimum recoil atom concentrations that degrade the insulating performance have not been examined. However, even if the recoil Fe and Cr atoms degrade the insulation performances in the regions of ~1.2 μ m from both the boundaries, coating layers adequately thicker than ~2.4 μ m, e.g., ~3 μ m thick coating, could maintain the insulating performance because the recoil atoms cannot reach the center region of the layer. The present discussions assume that positions of injected recoil metal atoms are fixed without diffusion and particle collisions. After studying the behaviors of the injected metal atoms at high temperatures under irradiation and the minimum concentrations that affect the insulating performance in the future experiments, thinner coating layers could be acceptable as the MHD insulating layer.

9. Summary

The development of ceramic insulating materials is being conducted to suppress the MHD pressure drop in advanced liquid metal blanket systems. The recent design investigations have provided the requirements for the MHD insulators and irradiation environments in the DEMO relevant conditions.

The electrical insulating performances of oxide plates, oxide coatings, and SiC plates have been examined. The conductivities of the examined oxide materials and SiC materials increased to 10^{-4}–

10^{-6} S/m and 10^{-1}–10^{1} S/m, respectively, at 500–700 ℃ regardless of the conductivities at room temperature. Since the results of a series of irradiation experiments indicate that the maximum magnitudes of radiation induced conductivities (RICs) would be ~10^{-6} S/m in oxide materials and <~1× 10^{-5} S/m in sintered SiC materials under the dose rates of several kGy/s at the first walls of blanket modules, respectively, and the magnitudes are almost independent of temperature, the conductivities of the MHD insulators in the blanket systems are considered to be dominated by thermal excitation at the blanket temperature. The increases due to the RIC phenomenon would not be an issue in the development of the MHD insulators.

There are margins of 1–2 orders between the electrical conductivities obtained for the candidate MHD insulators and those required from blanket system design (10^{-2}–10^{-3} S/m for oxide materials and 100 S/m for SiC materials). Various irradiation experiments are required to examine whether the margins can be maintained after irradiation of ~100 dpa in the future studies. In addition to the irradiation damage, the injection of recoil Li from the liquid metal coolants might be an issue for maintaining the insulating performances of the MHD insulation coatings.

CRediT authorship contribution statement

Teruya Tanaka: investigation, formal analysis, writing - original draft. Takumi Chikada: investigation. Tatsuya Hinoki: investigation. Takeo Muroga: investigation.

Declaration of competing interest

The authors declare that they have no known competing financial interests or personal relationships that could have appeared to influence the work reported in this study.

Acknowledgement

The corresponding author would like to thank Mr. K. Takeuchi from Nagoya University for the acquisition of the insulating performances of the MOD MgO coatings. The performance data on the MgO coatings, etc. has been obtained under the research program UFFF021 of National Institute for Fusion Science. The investigation of the recoil atom injection into ceramic coatings has been performed under the support of Japan Society for the Promotion of Science KAKENHI Grant-in-Aid for Scientific Research (B) 22H01209.

References

[1] D. L. Smith, et al., J. Nucl. Mat., 307–311 (2002) 1314–1322.

[2] T. Muroga, et al., Fusion Eng. Des. 85 (2010) 1301–1306.

[3] T. Chikada, et al., Comprehensive Nuclear Materials (Second Edition) 6 (2020) 274-283.

[4] M. Kondo, et al., Comprehensive Nuclear Materials (2nd edition) 6 (2020) 176–202.

[5] E. Mas de les Valls, et al., Journal of Nuclear Materials 376 (2008) 353–357.

[6] S. Tanaka, et al., Fusion Engineering and Design 51–52 (2000) 299–307.

[7] M. Enoeda, et al., Fusion Engineering and Design 81 (2006) 415–424

[8] A. Sagara, et al., Fusion Science and Technology, 47 (2005) 524–529.

[9] A. Sagara, et al., Fusion Engineering and Design 87 (2012) 594–602.

[10] J. Miyazawa, et al., Plasma and Fusion Research 12 (2017) 1405017.

[11] T. Murase, et al., Fusion Engineering and Design 136 (2018) 106–110.

[12] STREAM code manual, Cradle Co. Ltd. in Japan.

[13] S Smolentsev, et al., Fusion Engineering and Design 73 (2005) 83–93.

[14] K. Miyazaki, et al, Fusion Technology, 19 (1991) 969–975.

[15] H. Hashizume, Fusion Engineering and Design 81 (2006) 1431–1438.

[16] K. Okano, et al., Fusion Engineering and Design 136 (2018) 183–189.

[17] K. Tobita, et al., Fusion Science and Technology 75 (2019) 372–383.

[18] Y. Someya, et al., Fusion Engineering and Design 146 (2019) 894–897.

[19] T. Tanaka, et al., presented at 2021 Fall Meeting of the Atomic Energy Society of Japan, Sept. 8-10,2021. (Details are planned to be submitted to Plasma and Fusion Research.)

[20] K. Miyazaki, et al., Fusion Technology 10 (1986) 830-836.

[21] I.R. Kirillov, et al., Fusion Engineering and Design 27 (1995) 553–569.

[22] S. Smolentsev, et al., Fusion Engineering and Design 85 (2010) 1196–1205.

[23] S. Smolentsev, et al., Fusion Science and Technology 50 (2006) 107–119.

[24] T. Muroga, Comprehensive Nuclear Materials 4 (2012) 691–699.

[25] T. Hinoki, et al., Materials Transactions 54 (2013) 472–476.

[26] R. Norizuki, et al., Fusion Engineering and Design 168 (2021) 112438.

[27] M. Kondo, et al., presented at 20th International Conference on Fusion Reactor Materials (ICFRM-20) online, C123, Oct. 24-29, 2021.

[28] T. Tanaka, et al., Fusion Engineering and Design 88 (2013) 2569– 2572.

[29] T. Tanaka, et al., Journal of Nuclear Materials 455 (2014) 630–634.

[30] T. Nozawa, et al., Journal of Nuclear Materials 511 (2018) 582–590.

[31] T. Hinoki, et al., presented at 20th International Conference on Fusion Reactor Materials (ICFRM-20) online, I415, Oct. 24-29, 2021.

[32] T. Tanaka, et al., Journal of Plasma and Fusion Research SERIES, 9 (2010) 282–287.

[33] T. Tanaka, et al., Journal of Nuclear Materials, 367–370(2007)1155–1159.

[34] V. A. J. van Lint et al., “Mechanisms of Radiation Effects in Electronics Materials Vol. 1”, John Wiley ＆Sons, Inc., 1980.

[35] M. Rogalla, et al., Nuclear Physics B 78 (1999) 516-520.

[36] M. Abdou, et al., Fusion Engineering and Design 100 (2015) 2–43.

[37] D. B. Pelowitz, et al., MCNP6 User’s manual, LA-CP-13-00634.

[38] G. F. Knoll, “Radiation Detection and Measurement”, WILEY.

[39] R. C. Hughes, Physical Review B 19 (1979) 5319.

[40] G.P. Pells, Journal of Nuclear Materials 155–157 (1988) 67–76.

[41] R.W. Klaffky, et al., Physical Review B 21 (1980) 3610–3634.

[42] G.P. Pells, J. Nucl. Mater. 184 (1991) 177–182.

[43] E.R. Hodgson, J. Nucl. Mater. 212-215 (1994) 1123–1127.

[44] D.P. White, et al., J. Appl. Phys. 83 (1998) 1924–1930.

[45] T. Tanaka, et al., Fusion Engineering and Design 75–79 (2005) 933–937.

[46] T. Tanaka *et al*., Fusion Engineering and Design 66-68 (2003) 837–841

[47] T. Nishitani *et al*., 12th IEA Workshop on Radiation Effects in Ceramic Insulators, Helsinki, 11th Sep. 2002 (22nd SOFT Satellite Meeting).

[48] A.E. Costley, et al., Fusion Engineering and Design 55 (2001) 311–346.

[49] D.W. Muir, et al., “The NJOY Nuclear Data Processing System”, LA-UR-12-27079,2012.

[50] T. Shikama, et al., Journal of Nuclear Materials 258±263 (1998) 1867–1872

[51] L.L. Snead, et al., Journal of Nuclear Materials 226 (1995) 58–66.

[52] Hodgson, 13th IEA Workshop on Radiation Effects in Ceramic Insulators, Kyoto, 9th December 2003. (ICFRM-11 Satellite Meeting), JAERI-Review, 2004–004

[53] Hodgson, Journal of Nuclear Materials 191-194 (1992) 552–554.

[54]Y. Yasuda, et al., Journal of Nuclear Materials 329–333 (2004) 1451–1455.

[55] Y. Katoh, et al., Journal of Nuclear Materials 386–388 (2009) 639–642.

[56] T. Tanaka, et al., Fusion Engineering and Design 83 (2008) 1300–1303.

[57] H. Fujiwara, et al., presented at 20th International Conference on Fusion Reactor Materials (ICFRM-20) online, W_PS_1_C+D+I, #180,, Oct. 24-29, 2021.

[58] S. Kondo et al., Acta Materialia 83 (2015) 1–9.

[59] T.J. Dolan, et al., Fusion Technol. 26 (1994) 1014–1020.

[60] M. Fleming, et al., “The FISPACT-II User Manual”, UKAEA-R(18)001, 2018.

[61] R.L. Klueh, et al., Journal of Nuclear Materials 280 (2000) 353-359.

[62] http://www.srim.org/

[63] T. Sato, et al., Journal of Nuclear Science and Technology, 55 (2018) 684-690.

[64] R. Norizuki, et al., Fusion Engineering and Design 168 (2021) 112438.

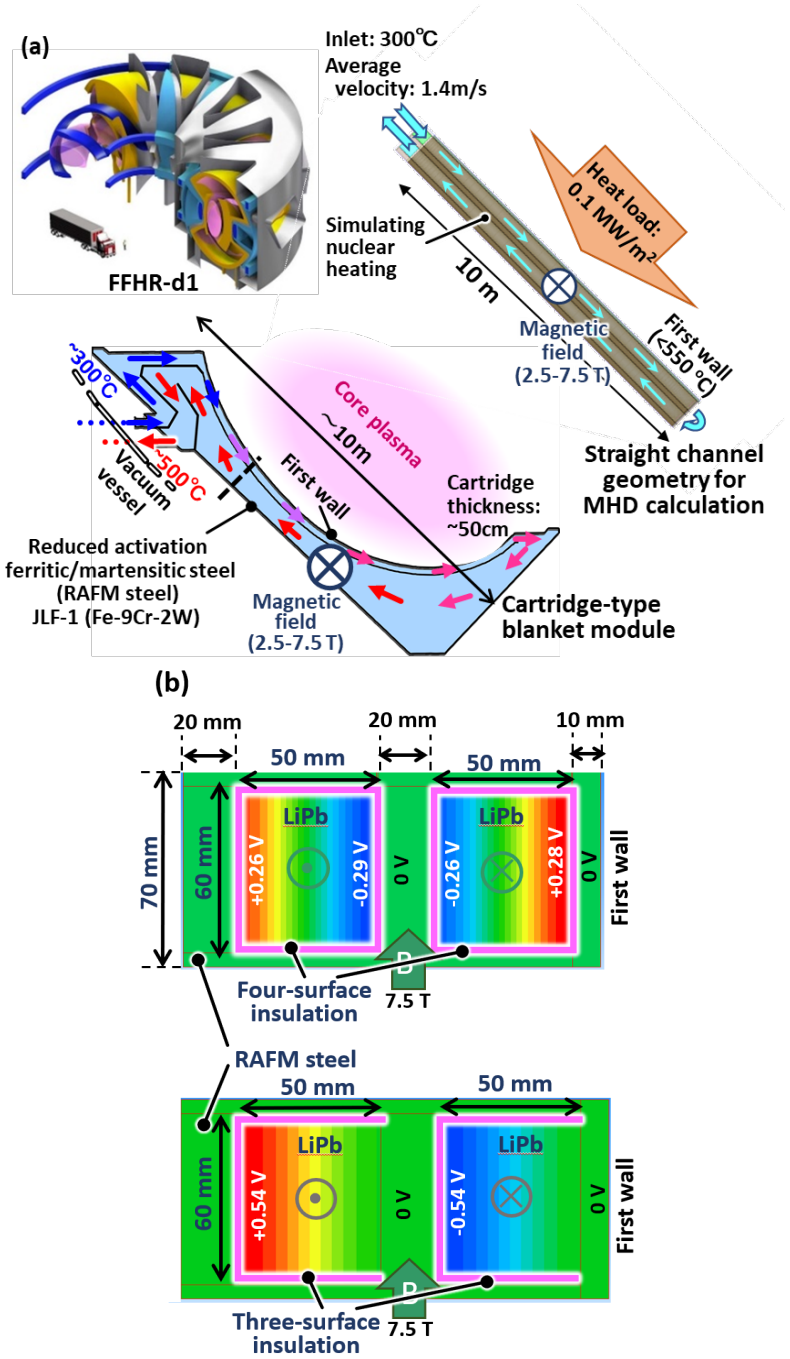

Fig. 1. (a) Cross section of cartridge-type LiPb blanket module investigated for FFHR-d1 [9-11] and straight channel geometry for MHD calculation of LiPb breeder/coolant flow. (b) Calculated electrical potential distribution in coolant channels with four-surface and three-surface insulation.

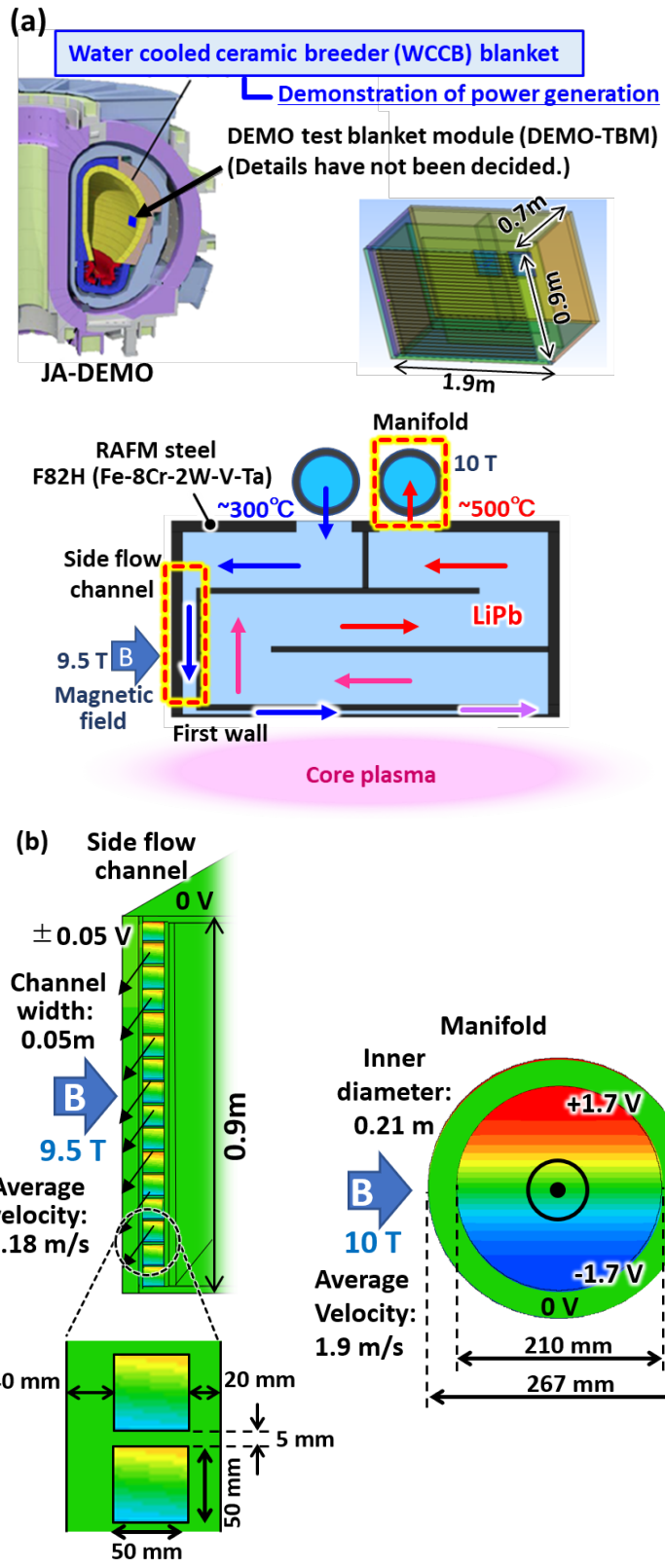

Fig. 2. (a) Tentative proposal of self-cooled LiPb JA-DEMO TBM.[17-19] (b) Calculated electrical potential distribution in the side flow channel and manifold.

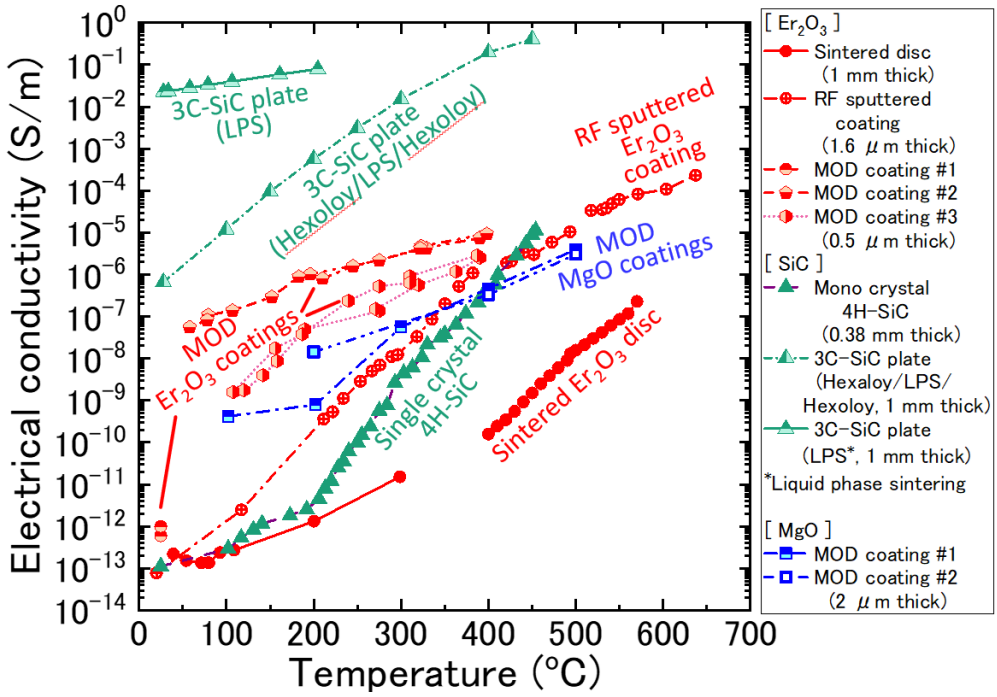

Fig. 3. Examples of temperature dependence of electrical conductivities of MHD insulator materials from Refs. 28, 32 and 33. Data for MOD MgO coatings were newly obtained.

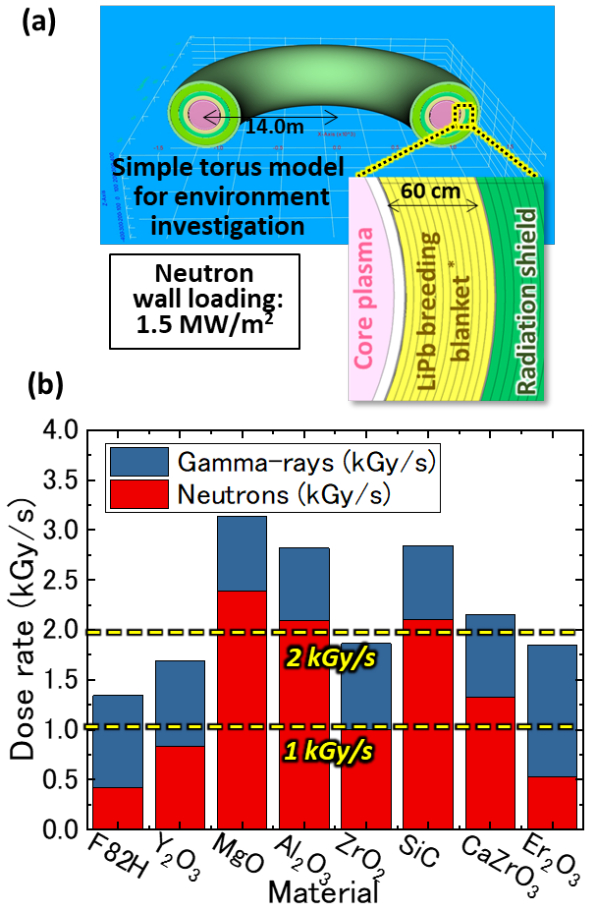

Fig. 4. (a) Simple torus model used for evaluation of neutron and gamma-ray irradiation environment. (b) Dose rates at first walls calculated for F82H (reduced activation ferritic/martensitic steel) and candidate MHD insulating materials.

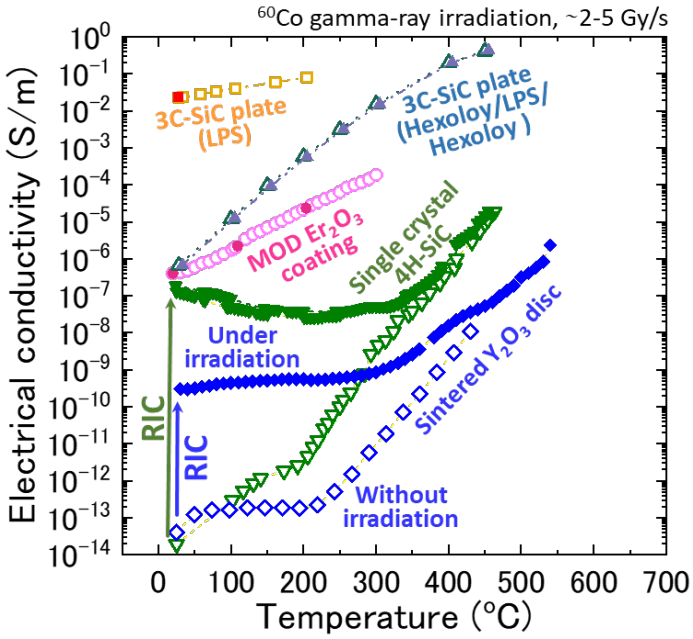

Fig. 5. Electrical conductivities of Y_2O_3 and SiC materials at room temperature and high temperatures under and without gamma-ray irradiation [32, 33]. Increases in conductivities under irradiation correspond to radiation induced conductivities (RICs) due to radiation excitations.

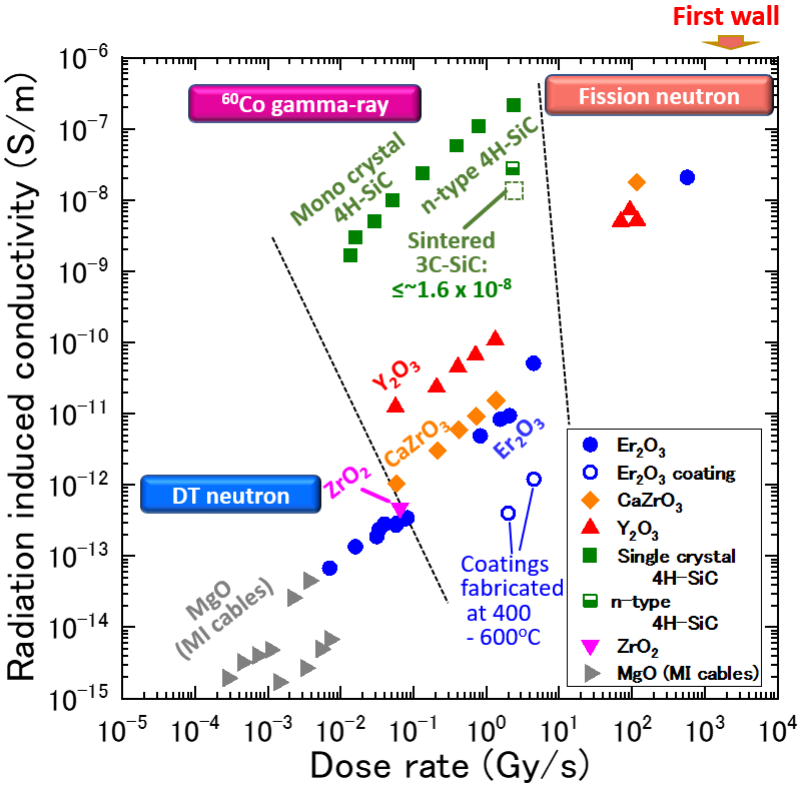

Fig. 6. Dose rate dependence of radiation-induced conductivities (RICs) in candidate MHD insulating materials at low temperatures (< 50℃) [28, 32, 33, 45–47]. The plot for a ZrO_2 plate was newly obtained. All data were evaluated in a vacuum to suppress background electrical currents due to ionized atmospheric gases except for fission reactor irradiation.

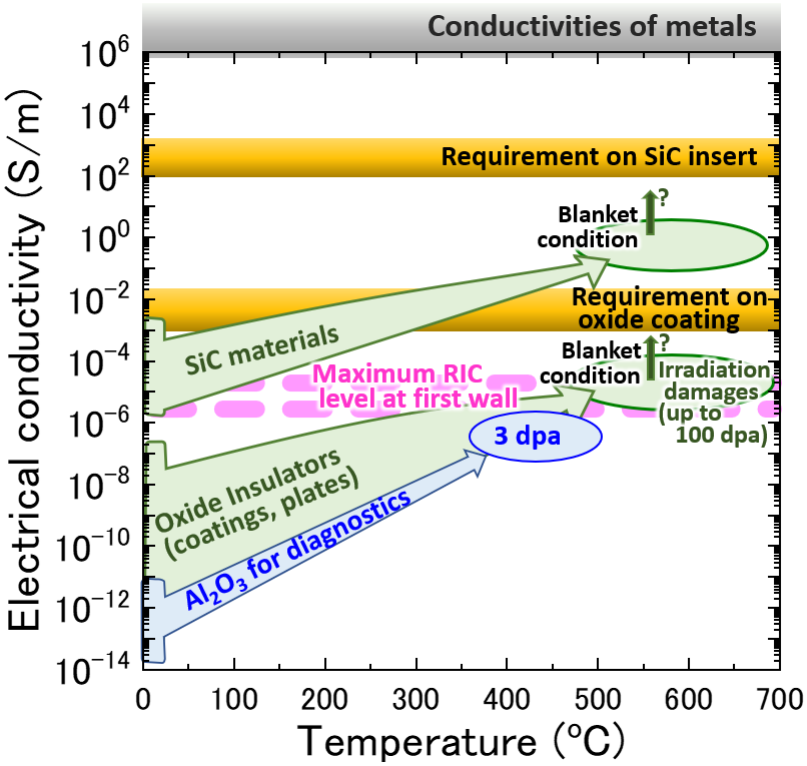

Fig. 7. Illustration of required insulating performances, increases in conductivities due to temperature and radiation induced conductivity (RIC) phenomenon in DEMO relevant condition. At the start of use in a blanket module, there would be margins of 1-3 orders in both oxide and SiC materials.

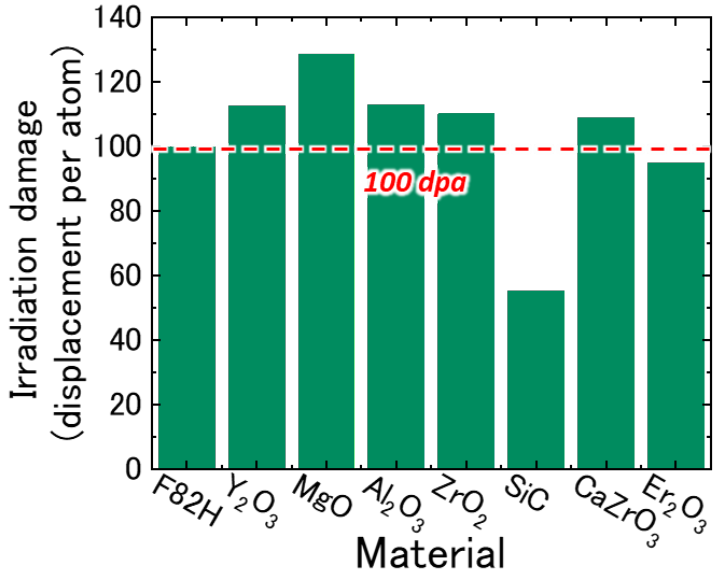

Fig. 8. Calculated irradiation damages at first wall. Assumed displacement energy and efficient factor are 40 eV and 0.8 except for SiC with the displacement energy of 28 eV.

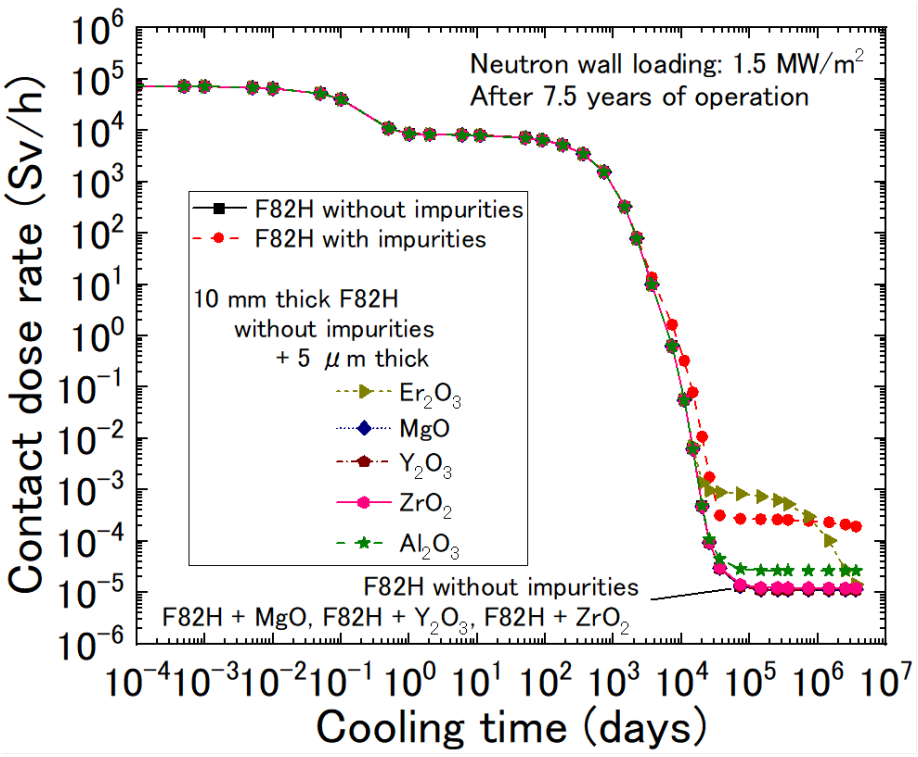

Fig .9. Contact dose rates of F82H and 10 mm thick F82H + 5-μm thick coatings calculated for impact evaluation of radioactivation.

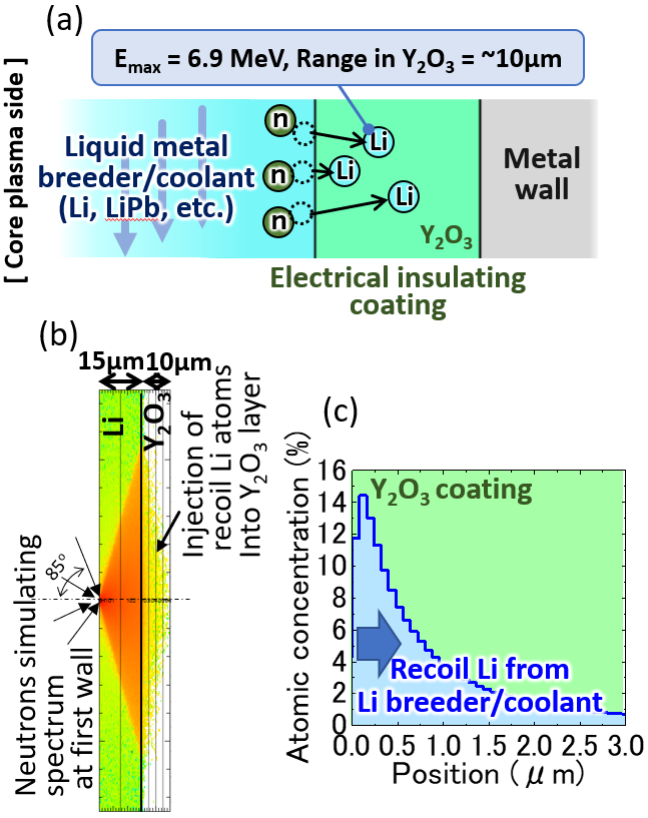

Fig. 10. (a) Injection of recoil Li atoms from coolants by 14 MeV neutrons. (b) Example of distribution of recoil Li atoms calculated using PHITS code. (c) Profile of initial positions of injected Li atoms. Concentration after 7.5 years of operation is estimated by assuming that positions of injected Li atoms are fixed without diffusion and collisions under irradiation.

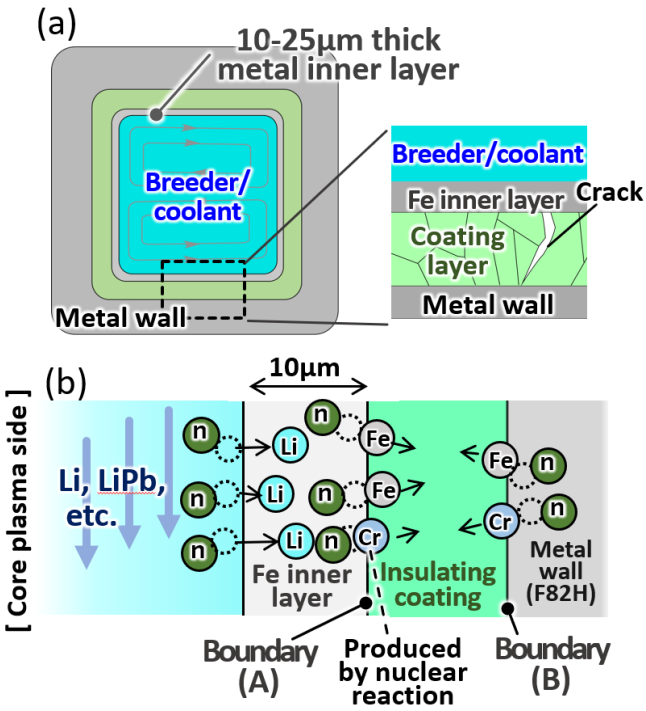

Fig. 11. (a) Attachment of metal inner layer proposed as penetration barrier for liquid metal through cracks [15] and as anti-corrosion barrier [64]. (b) Elimination of recoil Li atom injection by the Fe inner layer. Injection of recoil metal atoms from the Fe inner layer and metal wall into insulating coating is also drawn.